GLOBAL BIOGEOCHEMICAL CYCLES, VOL. 9, NO. 4, PAGES 541–556, DECEMBER 1995

On the contribution of CO_2 fertilization to the missing biospheric sink

P. Friedlingstein, [1] I. Fung, [1] E. Holland, [2] J. John, [1] G. Brasseur, [2]
D. Erickson, [2] and D. Schimel [2]

Abstract. A gridded biospheric carbon model is used to investigate the impact of the atmospheric CO_2 increase on terrestrial carbon storage. The analysis shows that the calculated CO_2 fertilization sink is dependent not just on the mathematical formulation of the "β factor" but also on the relative controls of net primary productivity (NPP), carbon residence times, and resource availability. The modeled evolution of the biosphere for the period 1850–1990 shows an increasing lag between NPP and the heterotrophic respiration. The time evolution of the modeled biospheric sink (i.e., difference between enhanced NPP and enhanced respiration) does not match that obtained by deconvolution of the ice core CO_2 time series. Agreement between the two is reasonable for the first half of the period, but during the recent decades the deconvoluted CO_2 increase is much too fast to be explained by the CO_2 fertilization effect only. Therefore other mechanisms than CO_2 fertilization should also contribute to the missing sink. Our results suggest that about two thirds to three fourths of the 1850–1990 integrated missing sink is due to the CO_2 greening of the biosphere. The remainder may be due to the increased level of nitrogen deposition starting around 1950.

Introduction

The global budget of carbon is presently poorly understood, with the greatest uncertainty focused on the size and location of the "missing CO_2 sink". The most recent estimations of the 1980s emission from fossil fuel burning (5.4 ± 0.5 Gt C/yr) [*Andres et al.*, 1995] and land use modification (1.6 ± 1.0 Gt C/yr) [*Houghton*, 1993] on the one hand, atmospheric CO_2 increase (3.2 ± 0.2 Gt C/yr) [*Keeling et al.*, 1995] and oceanic uptake (2.0 ± 0.5 Gt C/yr) [*Sarmiento*, 1993] on the other, lead to a CO_2 imbalance of 1.8 ± 1.2 Gt C/yr. That imbalance, integrated over the industrial period, amounts to about 100 Gt C.

Several recent modeling efforts to infer CO_2 source and sink distribution from atmospheric CO_2 concentration all suggest a strong net sink in the northern hemisphere mid latitudes [*Keeling et al.*, 1989b; *Tans et al.*, 1990; *Enting et al.*, 1993]. The partitioning between the ocean and the biosphere for this sink is highly controversial. Measurements of atmospheric and oceanic ^{13}C provide additional constraints on the distribution of the partitioning of the sink [*Keeling et al.*, 1989a; *Quay et al.*, 1992; *Ciais et al.*, 1995]. However, the uncertainties surrounding these constraints remain large [e.g., *Tans et al.*, 1993; *Francey et al.*, 1995].

Several processes can contribute to this unbalanced or missing sink. These include CO_2 fertilization, the impact of climatic variability on air-land and air-sea CO_2 exchange processes [*Dai and Fung*, 1993; *Keeling et al.*, 1995], and nitrogen deposition on land and ocean [*Peterson and Melillo*, 1985; *Schindler and Bayley*, 1993; *Hudson et al.*, 1994; *Townsend et al.*, 1995].

The fertilization effect, that is, the positive response of terrestrial biosphere to increasing atmospheric CO_2, is often cited as the major mechanism to explain the missing CO_2 sink [*Intergovernmental Panel on Climate Change (IPCC)*, 1990; 1992]. To estimate this contribution, we use a biospheric carbon model to calculate the time evolution of biospheric fluxes and pools under an atmosphere with increasing CO_2.

Formulation of CO_2 Fertilization Effect

The positive response of photosynthesis to increasing atmospheric CO_2 concentration has a strong experimental support [*Strain and Cure*, 1985; *Bolin et al.*, 1986; *Bazzaz*, 1990; *Mooney et al.*, 1991; *Körner and Arnone*, 1992; *Norby et al.*, 1992; *Wullschleger et al.*, 1995]. Most of the biospheric carbon cycle models, used to investigate the contemporary CO_2 budget, take

[1] NASA/Goddard Institute for Space Science, New York.
[2] National Center for Atmospheric Research, Boulder, Colorado.

Paper number 95GB02381.
0886-6236/95/95GB-02381$10.00

into account this effect, but the magnitude of the effect greatly differ because of the representation adopted. The differences arise, at least, at three levels: the physical variable stimulated by the atmospheric CO_2, the mathematical relation between this variable and the atmospheric CO_2, and the spatial variability of this relation.

First, the physiological quantity which is stimulated by the enhanced CO_2 is taken, in these models, to be either net ecosystem production (NEP) [e.g., *Keeling et al.*, 1989a], net primary production (NPP) [e.g., *Goudriaan and Ketner*, 1984; *Kohlmaier et al.*, 1987; *Esser*, 1987; *Polglase and Wang*, 1992], or gross primary production (GPP) [e.g., *Raich et al.*, 1991; *Warnant et al.*, 1994; *Sellers et al.*, 1995].

For example, *Keeling et al.* [1989a] proposed the following set of equations for the fertilization effect:

$$\Delta NPP = NPP_0[\beta_a \frac{C_t - C_0}{C_0} + \beta_b' \frac{B_t - B_0}{B_0}] \quad (1)$$

$$\Delta RES = NPP_0[\beta_b \frac{B_t - B_0}{B_0}] \quad (2)$$

where, respectively, NPP_0, C_0, and B_0 denote the unperturbed biospheric flux, and the unperturbed atmospheric and biospheric reservoirs; C_t and B_t denote the corresponding reservoir during the perturbation; and β_{NEP}, β_b, and β_b' are the first-order perturbation factors. The fertilization flux, F_{FER} is given by

$$F_{FER} = \Delta NPP - \Delta RES = NPP_0[\beta_{NEP} \frac{C_t - C_0}{C_0}] \quad (3)$$

β_b, and β_b' being chosen to be equal to 1. In other words, the β factor is applied, in effect, to NEP. We shall call this the β_{NEP} approach.

Another common formulation, the β_{NPP} approach, [e.g., *Goudriaan and Ketner*, 1984; *Esser*, 1987; *Polglase and Wang*, 1992] is

$$\Delta NPP = NPP_0[\beta_{NPP} \frac{C_t - C_0}{C_0}] \quad (4)$$

$$\Delta RES = k[B_t - B_0] \quad (5)$$

$$F_{FER} = NPP_0[\beta_{NPP} \frac{C_t - C_0}{C_0}] - k[B_t - B_0] \quad (6)$$

We have assumed, in (4), the same linear relation between atmospheric CO_2 and productivity as *Keeling et al.* [1989a], and, in (5), a first-order reaction rate for the respiration flux (i.e., the respiration is proportional to the biomass reservoir). Here, k, defined as NPP_0/B_0, is the turnover time of carbon in the biosphere.

It can be shown that the β_{GPP} approach is mathematically identical to the β_{NPP} if autotrophic respiration is proportional to NPP and/or to the biomass.

The β_{NEP} approach assumes that the relative increase of the net biospheric CO_2 flux (NEP) is proportional the the relative increase of the atmospheric CO_2 concentration, whereas the β_{NPP} approach assumes that it is the NPP flux which has a growth proportional to CO_2.

To illustrate the implications of these two methods, we assume a linear increase in atmospheric CO_2, that is, $C_t = C_0(1 + \Gamma t)$. The β_{NEP} formulation gives

$$F_{FER} = \frac{\partial B}{\partial t} = NPP_0 \beta_{NEP} \Gamma t \quad (7)$$

$$B - B_0 = NPP_0 \beta_{NEP} \Gamma t^2/2 \quad (8)$$

$$\Delta NPP = NPP_0 \beta_{NEP} \Gamma (t + kt^2/2) \quad (9)$$

$$\Delta RES = NPP_0 \beta_{NEP} \Gamma k t^2/2 \quad (10)$$

The β_{NPP} formulation leads to

$$F_{FER} = \frac{\partial B}{\partial t} = NPP_0 \beta_{NPP} \frac{\Gamma}{k}(1 - e^{-kt}) \quad (11)$$

$$B - B_0 = NPP_0 \beta_{NPP} \frac{\Gamma}{k^2}[kt - (1 - e^{-kt})] \quad (12)$$

$$\Delta NPP = NPP_0 \beta_{NPP} \Gamma t \quad (13)$$

$$\Delta RES = NPP_0 \beta_{NPP} \frac{\Gamma}{k}[kt - (1 - e^{-kt})] \quad (14)$$

One striking difference between the two approaches is that the biomass will increase quadratically with time in the β_{NEP} formulation (8), that is to say, faster than the atmospheric CO_2 increase. Conversely, the β_{NPP} approach will have a slower than linear biomass growth (12). The negative exponential term in (12) expresses the lag of the respiration flux, which is explicitly dependent on the biomass turnover time $(1/k)$.

Similarly, the net biospheric uptake, F_{FER}, is designated to follow the atmospheric CO_2 increase in the β_{NEP} approach (7), and so will have unimpeded growth. By contrast, (11) clearly shows that the biospheric sink will reach, at large t, a constant value $(NPP_O \beta_{NPP} \Gamma/k)$ in the β_{NPP} case. This is due to the fact that, as the CO_2 increase is linear, the respiration flux growth eventually catches up the NPP flux growth. This behavior is illustrated in Figure 1a. Note that the two approaches become identical for $k \to 0$, that is to say, the β_{NEP} approach implicitly assumes an infinite biospheric carbon turnover time.

It is therefore obvious that the numerical value of β is dependent on the method adopted. Figure 1 clearly shows that to achieve a specified biospheric sink (such as the flux needed to balance the present-day CO_2 budget), the β_{NPP} case will require a higher value for β than the β_{NEP} case does. Indeed, the β_{NEP} is, by definition, constant in the β_{NEP} case, but it decreases

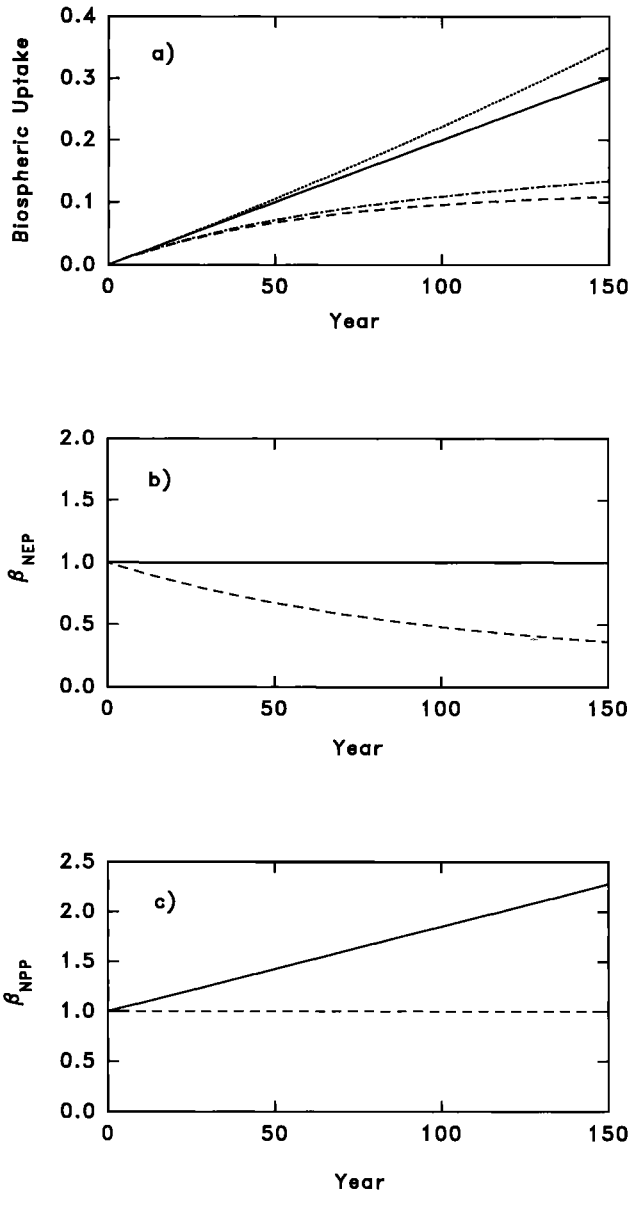

Figure 1. (a) Time evolution of biospheric uptake obtained with the β_{NEP} (solid line) and β_{NPP} (dashed line) formulations for a linear atmospheric CO_2 increase (see (7) and (11)). Dotted line and dash-dotted line are for an exponential atmospheric CO_2 increase. (b) Time evolution of β_{NEP} in a β_{NEP} formulation (solid line) and in a β_{NPP} formulation (dashed line). (c) same as (b) but for β_{NPP}.

exponentially with time in the β_{NPP} based formulation (Figure 1b). Conversely, the β_{NPP} which is constant in a β_{NPP} approach, increases linearly with time in the β_{NEP} based formulation (Figure 1c).

It can be shown that the use of a more realistic exponential atmospheric CO_2 time evolution, in place of the illustrative linear CO_2 trend we adopted, does not affect qualitatively the results. The difference between the biospheric uptake estimated when the atmospheric forcing is linear or exponential is illustrated in Figure 1a. As the growth rate of the atmospheric CO_2 ($\Gamma \simeq 0.002\ \mathrm{yr}^{-1}$) is still relatively small compared to the inverse of the characteristic time of the carbon in the biosphere ($k \simeq 1/60\ \mathrm{yr}^{-1}$), there is only minor differences between the biospheric responses to an exponential or a linear atmospheric CO_2 increase.

A second important source of confusion among models comes from the mathematical formulation adopted for the fertilization function. Complexity ranges from the linear function, as shown hereinabove (4), or the logarithmic β function first introduced by *Bacastow and Keeling* [1973]:

$$P_t = P_0[1 + \beta_{log} \ln(\frac{C_t}{C_0})] \tag{15}$$

to the more elaborate Michaelis-Menten expression [e.g., *Farquhar et al.*, 1980; *Gates*, 1985; *Gifford*, 1992]:

$$P_t = P_0 \frac{K_1(C_t - C_b)}{1 + K_2(C_t - C_b)} \tag{16}$$

where

$$\begin{aligned} K_1 &= [1 + K_2(C_0 - C_b)]/[C_0 - C_b] \\ K_2 &= \frac{(2C_0 - C_b) - r(C_0 - C_b)}{(r-1)(C_0 - C_b)(2C_0 - C_b)} \\ r &= P_{2\times CO_2}/P_{1\times CO_2} \end{aligned}$$

where P_0 and P_t are the productivity fluxes (GPP, NPP, or NEP) for a C_0 and a C_t atmospheric CO_2 concentration, respectively. β_{log} is a constant factor, it expresses the relative increase of productivity for an atmospheric CO_2 increase.

The Michaelis-Menten (hyperbolic) formulation is the most realistic as it leads to a zero NPP for $C = C_b$, the CO_2 compensation point; and it saturates to K_1/K_2 when atmospheric CO_2 tends to infinity. Also, r, the NPP increase for a doubling of the CO_2 concentration, can easily be related to β. For example, one can calculate the r_{log}, the equivalent r of the logarithmic form:

$$r_{log} = 1 + \ln(2)\beta_{log} \tag{17}$$

As we will show below, the choice of linear, logarithmic or hyperbolic function is not crucial for the industrial time period. Within the 280 to 350 ppmv interval, the biospheric uptakes estimated with these three formulations have very similar time evolution. However, the numerical value of β needed to achieve a given uptake is again dependent on the mathematical formulation adopted: the logarithmic form requires a higher value for β than the linear form does. Therefore it is crucial to explicitly mention the formulation used as well as the physiological variable it is applied to when one makes use of a β formulation.

Finally, one has to make some assumptions about the geographical distribution of the fertilization effect. Studies dedicated mainly to the analysis of the atmospheric CO_2 signal usually choose one of the β function described before, assume a constant β, but allow the spatial distribution of the fertilization sink to follow a prescribed NPP spatial distribution [*Heimann and Keeling,* 1989; *Tans et al.,* 1990; *Enting et al.,* 1993]. Many biospheric models [e.g., *Goudriaan and Ketner,* 1984; *Esser,* 1987; *Kohlmaier et al.,* 1989; *Polglase and Wang,* 1992] also assume a uniform β (that is to say, the relative productivity increase is a function of atmospheric CO_2 only). Indeed, results from experiments show that, whereas the NPP is strongly affected by environmental stresses such as extreme temperatures, light, water and nutrient limitations, the relative increase of NPP under enhanced CO_2 conditions is primarily independent of these stresses [*Wullschleger et al.,* 1995].

However, the opposite conclusion is given by other experiments. They show that the relative NPP increase is very sensitive to the availability of environmental variables other than CO_2 [*Oechel and Strain,* 1985; *Gifford,* 1992; *Körner,* 1993; *Oechel et al.,* 1994]. Impact of increased CO_2 on plant water use efficiency (WUE) [*Gifford,* 1992; *Polley et al.,* 1993], long-term nutrient availability and carbon allocation [*Vitousek and Howarth,* 1991; *Gifford,* 1992] may modulate the relative response of the different ecosystems.

Physiological models [*Woodward and Smith,* 1995], or process-based models [*Melillo et al.,* 1993], accounting for the major feedbacks between CO_2 water and nutrient, seem to estimate that the mean relative response of NPP to a doubling of atmospheric CO_2, is also vegetation-type dependent. Xeromorphic ecosystems have a higher relative response than mesic ecosystems, and cold climate ecosystems show the lowest relative response.

Methodology

At the moment, there is no definitive understanding, at an ecosystem level, of the long-term response of the biosphere to enhanced CO_2. Therefore in the following, we will carry out two types of numerical experiments: one assuming that the relative NPP increase (i.e., β_{NPP}) is spatially constant, and the second set of calculations with a relative NPP increase function of environmental limitations, that is to say, water and nutrients.

Model Description

The biospheric model we have developed, SLAVE (Scheme for Large Scale Atmosphere Vegetation Exchange), predicts on a 5° × 5° latitude/longitude resolution grid the global distribution of nine natural vegetation types, incorporates the effects of managed areas, and calculates the seasonal cycle of the main biospheric carbon pools and fluxes from climatic variables (Figure 2).

SLAVE contains five submodels: a vegetation scheme, a soil water budget submodel, a carbon scheme, a nutrient scheme, and a fertilization factor submodel. Here we will focus on the last two submodels, the first three having been described in earlier versions of the model [*Friedlingstein et al.,* 1992; 1994]

In our model, where NPP is calculated from climatic variables only, a physiological treatment of the fertilization effect is impossible. The NPP formulation we use [*Friedlingstein et al.,* 1992] is derived from the Miami model [*Lieth,* 1975]. Two empirical correlations were established by Lieth, the first relating measured NPP to mean annual temperature, the second relating measured NPP to mean annual precipitation. The Miami model assumes that for any combinations of temperature and precipitation, the NPP realized is given by the lesser value of the two correlations. As the NPP data

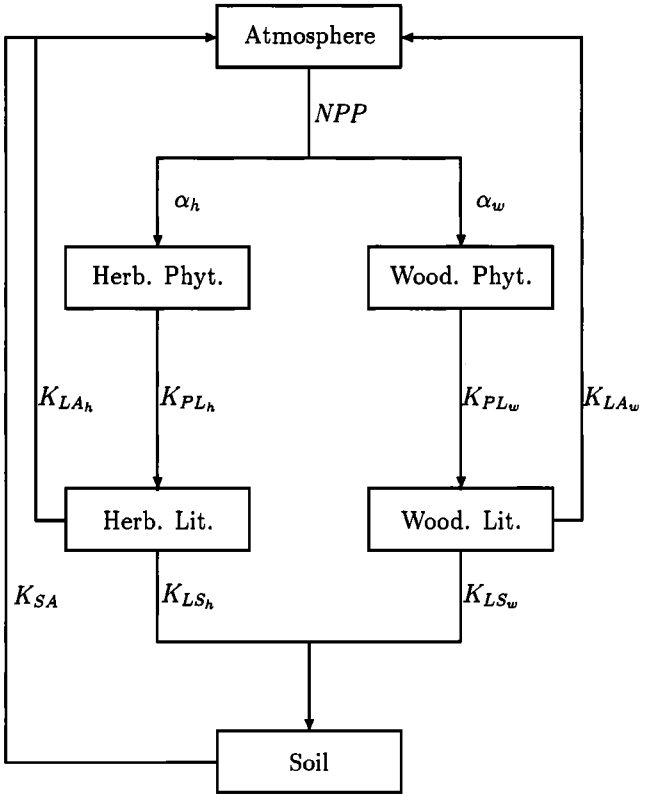

Figure 2. Schematic diagram of the biospheric model, Scheme for Large Scale Atmosphere Vegetation Exchange (SLAVE). NPP is partitioned into herbaceous and woody phytomass. Each of these pools supplies the litter compartments which return CO_2 to the atmosphere, a small fraction being sequestred in the soil pool. Decomposition rates are functions of vegetation type and climate [*Friedlingstein et al.,* 1992; 1994].

used to develop the correlation are in situ values, they account for all environmental limitations, including nitrogen, phosphorous, and other limitation. Similarly, if the CO_2 fertilization effect was operating in the 1950s (period of measurement) it is implicitly included in the regression relationships.

Our strategy is, therefore, to first calculate NPP as a function of the climate only, using our Miami-derived parametrization (representative of the late 1950s, that is, atmospheric CO_2 around 315 ppmv) and then to correct it for the actual atmospheric CO_2 level, using a Michaelis-Menten function (16) with the factor r (β) either constant or modulated by the water, and nutrient (nitrogen and phosphorus) availability.

To facilitate comparison with other studies, we kept the widely used parameter β for the model description and results discussion, r and β being related by (17). We need an estimate of the water, nitrogen, and phosphorous soil status in order to derive the fertilization effect as a function of the availability in these environmental variables.

Nitrogen subscheme. Plants assimilate mineral nitrogen available in the soil. This mineral nitrogen is produced during the microbial decomposition of soil organic matter. This process, called remineralization, is primarly controlled by the climatic conditions. Warm and wet conditions favour the bacterial activity and the remineralization of organic matter.

We developed a simple model of the mineral nitrogen in litter and soil pools. This submodel computes organic and mineral nitrogen available in litter and soil from climatic variables, vegetation type information, and the carbon content of litter and soil calculated by SLAVE.

We estimated $L_{N_{av}}$ and $S_{N_{av}}$, respectively, the mineral nitrogen available in litter and soil, in two steps: (1) we calculate, for optimal climatic conditions, the potential mineral nitrogen pools, $L_{N_{Pot}}$ and $S_{N_{Pot}}$; (2) temperature and water constraints are brought in to modulate these two pools.

$$L_{N_{av}} = L_{N_{Pot}} \times f_T \times f_{H_2O} \quad (18)$$

$$S_{N_{av}} = S_{N_{Pot}} \times f_T \times f_{H_2O} \quad (19)$$

The calculation of $L_{N_{pot}}$, the potential mineral nitrogen in the litter compartment, uses the equation from *Melillo et al.* [1983, 1984]:

$$L_{N_{pot}} = \left[\left(\frac{(100 - N_0(-28.48 - 0.91L_0))^2}{-4(-28.48 - 0.91L_0)}\right) - 100N_0\right] 10^{-4} \quad (20)$$

This parametrization deduces $L_{N_{pot}}$ (gram nitrogen immobilized per gram initial material) from two variables: the lignin content, L_0 (%), and the initial organic nitrogen content of the litter, N_0 (gram organic nitrogen per gram initial material). For each vegetation type, we specified a lignin content (Table 1) [*Melillo et al.*, 1982; 1983; 1984; *Pastor and Post*, 1986; *Parton et al.*, 1993]. Initial organic nitrogen is directly obtained from the litter carbon content calculated by SLAVE and a litter C:N ratio. This latter parameter, deduced from the literature, is vegetation type dependent (Table 1) [*Pastor and Post*, 1986; *Vitousek et al.*, 1988; *Schlesinger*, 1991; *Raich et al.*, 1991; *McGuire et al.*, 1992].

For the soil compartment, we assumed that potential mineral nitrogen amounts to 3 % of the soil organic nitrogen [*Parton et al.*, 1993]. As for litter, soil organic nitrogen is estimated from the calculated soil organic carbon divided by a soil C:N ratio (Table 1).

The temperature limiting function, f_T is a Q_{10} function ($Q_{10} = 2$):

$$\left.\begin{array}{ll} f_T = Q_{10}^{\frac{T-30}{10}} & \text{if } T < 30°C \\ f_T = 1 & \text{if } T > 30°C \end{array}\right\} \quad (21)$$

Here, f_{H_2O}, the water availability function, is equal to the ratio of precipitation (P) to potential evapotranspiration (PE). The lower limit of f_{H_2O} is set to 0.5,

Table 1. Parameters That are Vegetation-Type Dependent in the Nitrogen Budget Calculation of SLAVE

	Vegetation Type	L_0, %	$(C:N)_{veg}$	$(C:N)_{lit}$	$(C:N)_{soil}$
1,	evergreen tropical forest	10	50	50	15
2,	seasonal tropical forest	10	50	50	15
3,	savannah	10	40	40	15
4,	grassland / Shrubland	10	40	40	10
5,	temperate deciduous forest	10	50	60	20
6,	coniferous forest	25	50	70	20
7,	tundra	6	40	50	20
8,	desert and semidesert	6	40	50	20
9,	ice desert	6	40	50	20
10,	cultivation	10	40	40	10

reflecting the fact that mineralization is not dramatically affected by aridity (P. Vitousek, personal communication). When P/PE exceeds one, mineralization is not limited, except for inundated regions (P to PE ratio higher than two) where f_{H_2O} decreases linearly with P/PE.

Spatial Variability of β. As mentioned before, there is evidence that nutrients deficits (mainly mineral nitrogen and phosphorus) may limit the response of NPP to atmospheric CO_2 increase, whereas water deficits may enhance the CO_2 response [*Oechel and Strain*, 1985; *Mooney et al.*, 1991; *Körner*, 1993; *Oechel et al.*, 1994]. In this section, we describe the parameterization of β_{NPP} as a function of the levels of nitrogen, phosphorus, and water in the soil:

$$\beta_{rel} = f_W \times f_N \times f_P \quad (22)$$

$$\beta_{NPP} = \alpha_{calib} \times \beta_{rel} \quad (23)$$

Here, α_{calib} is a globally uniform scaling factor to be determined a posteriori, and f_W, f_N, and f_P are nondimensional scaling functions that respectively describe the dependence of β on water stress, nitrogen, and phosphorus availability.

We note that β_{NPP} (cf. (23)) is the parameter of importance in the determination of the magnitude of the CO_2 fertilization effect. In other words, f_W, f_N, and f_P can each be set to its own arbitrary scale independent of the others, as long as the determination of α_{calib} is self consistent with these scales. If (22) and (23) were applied in a one-dimensional model, the arbitrary scales would be irrelevant as they would have been incorporated into α_{calib}. The geographic distribution of β_{NPP} or β_{rel}, however, reflects the arbitary scales or relative importance of each of the factors: a factor whose values range between 0 and 100 will overwhelm a factor whose values range between 0.9 and 1.1. Lacking any definitive ranking of these factors across the entire landscape, we gave the three factors equal weighting by assigning them scales such that their ranges are of order 1. In this way, $f = 1$ means that the factor plays no role in modulating the CO_2 fertilization response, whereas $f < 1(>)$ limits (enhances) the CO_2 fertilization response.

We emphasize that these parametrizations should be viewed as an attempt to summarize hypotheses frequently made by ecophysiologists rather than an exact reproduction of the field data measurements. The parameterization of f_W, f_N, and f_P are described below. The response of CO_2 fertilization to water stress increases with increasing water stress [*Mooney et al.*, 1991; *Gifford*, 1992]. Stomatal density as well as stomatal conductance is expected to decrease under elevated CO_2 [*Woodward*, 1987a; *Bazzaz*, 1990]. Consequently, transpiration rate is expected to be reduced. In other words, water use efficiency (ratio of carbon gain to water loss) is expected to increase for elevated CO_2. Water stressed plants are expected to benefit more from this effect. It should be noted that reduced transpiration can lead to higher leaf temperature which may have a negative impact on NPP. However, under a constant climate, as we have assumed in this study, this effect is presumably of secondary importance. For future climate, with expected higher temperature, and especially, higher temperature extremes, the transpiration cooling reduction could lead to strong negative impact on NPP.

Here we parameterize the water use efficiency sensitivity as a nondimensional scaling function, f_W, which varies with PE/P, the potential evapotranspiration (PE) to precipitation (P) ratio (Figure 3a). When PE/P is lower than or equal to one, we assume that there is no

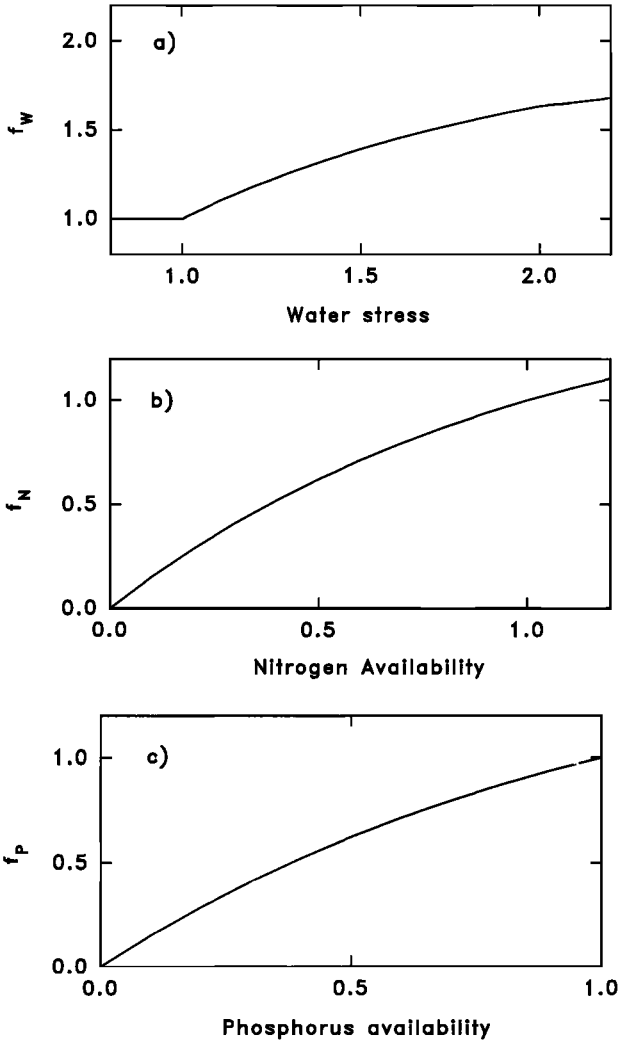

Figure 3. Relative CO_2 fertilization scaled as function of (a) water stress, (b) nitrogen availability, and (c) phosphorus availability. Abscises are (a) PE/P, (b) NPP_{Pot}/NPP_{Act}, and (c) fraction of 5°×5° grid cell free of ferralsol and acrisol. Ordinates are nondimensional arbitrary units for all functions.

water limitation, CO_2 fertilization proceeds at a rate independent of the water status, and $f_W = 1$. Also, f_W increases with increasing water stress (increasing PE/P) and the CO_2 fertilization response asymptotically saturates at $f_W = 2$ ($f_W = 2 - e^{(1-PE/P)}$).

The parameterization of the effect of nitrogen limitation on CO_2 fertilization is difficult, because there are few field or laboratory experiments that quantify this relationship. We assume that the nondimensional scaling function, f_N, is a monotonically increasing function of NPP_{Pot}/NPP_{Act}, where NPP_{Pot} is the maximum NPP attainable if all the mineral nitrogen in the litter and soil pools were available for photosynthesis, and NPP_{Act} is the NPP actually attained (see below). If $NPP_{Pot}/NPP_{Act} \ll 1$, all the nitrogen available is used already for photosynthesis, and no additional nitrogen is available to enhance photosynthesis. In this case, f_N tends to zero. For $NPP_{Pot}/NPP_{Act} = 1$, we assume that the fertilization response equates to 1 (Figure 3b).

We next need to estimate NPP_{Act} and NPP_{Pot}. We assume that NPP_{Act} is given by the Miami-derived NPP formulation [*Friedlingstein et al.,* 1992], which is rooted in field measurements of NPP. NPP_{Pot} is deduced from the available mineral nitrogen in the litter and soil reservoirs. For a given amount of mineral nitrogen, plants are able to fix limited amount of carbon. We calculated NPP_{Pot} as follows:

$$NPP_{Pot} = (L_{N_{av}} + S_{N_{av}})(C:N)_{veg} \qquad (24)$$

The available mineral nitrogen in the litter and soil pools, $L_{N_{av}}$ and $S_{N_{av}}$, are estimated using (18) and (19). Also, $(C:N)_{veg}$ is taken to be the C:N ratio of leaves and new wood, the first products of photosynthesis. These C:N ratios vary with vegetation types, and typically range from 50 for tropical to 100 for boreal ecosystems [*Pastor and Post,* 1986; *Vitousek et al.,* 1988; *Schlesinger,* 1991; *Raich et al.,* 1991; *McGuire et al.,* 1992]. Actually, this range already reflects the nitrogen limitation. Low nitrogen availability (as in high-latitude regions) induces an increase in the nitrogen use efficiency, that is, more carbon fixed by photosynthesis per nitrogen unit. In this model, where we try to estimate the nitrogen limitation, the use of this observed range of C:N ratios would bias the results, giving the solution of the problem a priori. To avoid this circularity, we made use of a low and constant C:N ratio representative of non N-limited regions for all vegetation types (Table 1).

Phosphorus is known to be very low in old tropical highly leached clay soils [*Vitousek and Sanford,* 1986; *Vitousek and Howarth,* 1991]. Being unable to evaluate mineral phosphorus as we did for nitrogen, we derived it, as a first approximation, from the soil database of *Zobler* [1986] compiled from the *Food and Agricultural Organization (FAO)* [1974-1982] soil taxonomy. Since tropical forests are primarily associated with ferralsols and acrisols [*Vitousek and Sanford,* 1986; *Bouwman,* 1990], we assumed that f_P, the phosphorus availability, is anticorrelated with the fraction of ferralsol and acrisol in each grid cell. Phosphorous is supposed to be non limiting in regions free of ferralsol or acrisol soil types (Figure 3c).

It should be noted that, unlike N and P, water limitation has a positive effect on fertilization, reflecting the increase of the water use efficiency. The three modulating functions, f_W, f_N, and f_P, (Figure 3) were assigned exponential shapes ($a + be^{-x}$), as it can expected that plant response should saturate when the limitation becomes negligible (for nutrients) or extremely large (for water).

Experiment Description

In this study, atmospheric CO_2 annually averaged for the period 1850–1990 were used as forcing for the fertilization function. We carried out six experiments, as described below (Table 2). All of these experiments make use of the temperature and precipitation climatology of *Shea* [1986], and the vegetation distribution of *Matthews* [1983] aggregated into 10 classes, nine natural vegetation types, and one cultivation class (see Table 1).

Table 2. Experiment Description: Shape, Spatial Distribution and Scaling Factor of β_{NPP}

Experiment	β Function [a]	β Distribution [b]	T_{calib} [c]
1	hyperbolic	constant	–
2	hyperbolic	f_W, f_N, f_P	1990
3	hyperbolic	f_W, f_N, f_P	1950
4	hyperbolic	f_W, f_N, f_P	1920
5	linear	f_W, f_N, f_P	1990
6	logarithmic	f_W, f_N, f_P	1990

[a] See equations 4, 15, and 16.
[b] See equation 22.
[c] See equation 25.

Experiment 1 employs a geographically uniform value for β ($\beta_{NPP} = 0.35$), a value adopted in the calculations of *Heimann and Keeling* [1989], *Tans et al.* [1990] and *Enting et al.* [1993]. Experiments 2-4 use the β dependence on water, nitrogen and phosphorus, as described above, using the hyperbolic formulation (16). As a sensitivity test, we also carried out experiments 5 and 6, to explore the linear and logarithmic functions (equations 4 and 15, respectively).

Siegenthaler and Sarmiento [1993] obtained the history of the missing sink as the residual in the atmospheric CO_2 increase, after contributions from fossil fuel combustion, land use modification, and oceanic uptake have been accounted for [*Siegenthaler and Sarmiento*, 1993]. The cumulative residual sink is 12, 31, and 97 Gt C for the periods 1850–1920, 1850–1950, and 1850–1990, respectively.

In our investigation, the residual missing sink for different periods is used to assess the magnitude of the CO_2 fertilization effect. This is described below.

The 1850 NPP for experiment 1 was obtained by uniformly scaling Miami NPP using (16). For the other experiments, an iterative procedure was carried out. The biospheric model was first integrated over 2000 years until preindustrial equilibrium with atmospheric CO_2 = 280 ppmv) was achieved. A year-to-year integration over the 1850–1990 period was then executed, with the model driven by the observed increasing atmospheric CO_2 and α_{calib} set to 1. The time integral of the biospheric sink was then used to scale the value of α_{calib}. This value was reintroduced in the initialization process and in the year-to-year integration, to derive a new value of α_{calib}, and so on until convergence. We postulate that CO_2 fertilization effect is the sole mechanism for the biospheric sink from 1850 up to some year T_{calib}, after which other factors may contribute to the sink as well. For any particular year T_{calib} (between 1850 and 1990), the scaling factor α_{calib} (23) can be adjusted in order to have

$$\int_{1850}^{T_{calib}} F_{FER}(t)\,dt = \int_{1850}^{T_{calib}} F_{MIS}(t)\,dt \qquad (25)$$

where $F_{FER}(t)$, the net biospheric uptake is the difference between NPP and the heterotrophical respiration flux calculated by SLAVE (Figure 2), and $F_{MIS}(t)$ is the residual missing sink obtained by *Siegenthaler and Sarmiento* [1993]. Over the whole time record (1850–1990), the integrated residual sink amounts to 97 Gt C.

In experiment 2, we choose $T_{calib} = 1990$, that is, the missing sink cumulated over the whole time series is due to the fertilization effect only. In experiments 3 and 4, hence, we used $T_{calib} = 1950$ and $T_{calib} = 1920$, respectively, to see whether CO_2 fertilization can explain the cumulative missing sink until 1990 with these alternate calibrations or there is room for other mechanisms to explain the missing sink.

By using the residual missing sink derived by *Siegenthaler and Sarmiento* [1993] as the benchmark, we are exploring the degree to which CO_2 fertilization can contribute to the missing sink, rather than the total magnitude of the missing sink itself.

Results

The net CO_2 flux from the atmosphere to the biosphere is the result of the imbalance between two perturbed fluxes: the increased NPP due to fertilization effect (uptake) versus the enhanced heterotrophic respiration from litter and soil due to the growth of these reservoirs (release). At equilibrium (1850), the fluxes are equal and the global NPP amounts to 56 Gt C/yr. The time evolutions of uptake (NPP) and release (RES) for experiment 1 (Figure 4), show an obvious difference between these two responses to the atmospheric CO_2 forcing: the increase in biospheric uptake is immediate, whereas the increase in the release is delayed. This delay is due to the turnover times of carbon in the phytomass, litter, and soil pools. With longer turnover times, the delay is larger. Tropical ecosystems are the most productive, but they have fast turnover times. High-latitude ecosystems exhibit opposite properties. As a result, the net biospheric sink is not a simple function of NPP only, but a subtle combination of NPP and turnover time. This is clearly shown in Figure 5, which represents the zonally averaged distributions of NPP and 1990 biospheric uptake from experiment 1

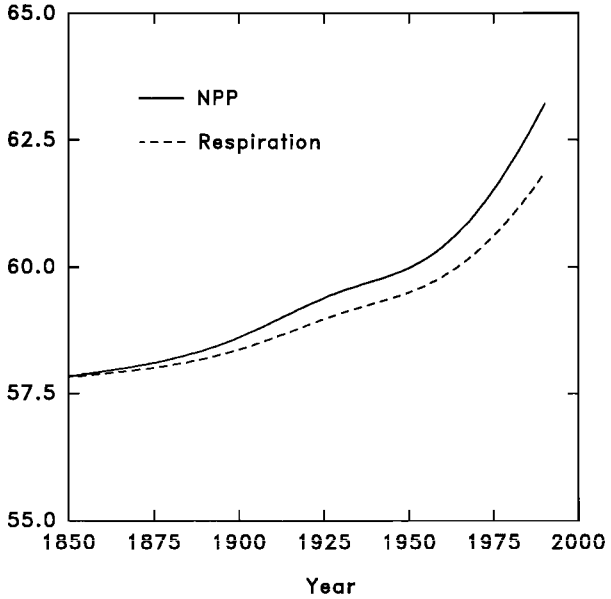

Figure 4. Modeled time evolution of global NPP (solid line) and heterotrophic respiration (dashed line) for experiment 2. Units are gigatons carbon per year.

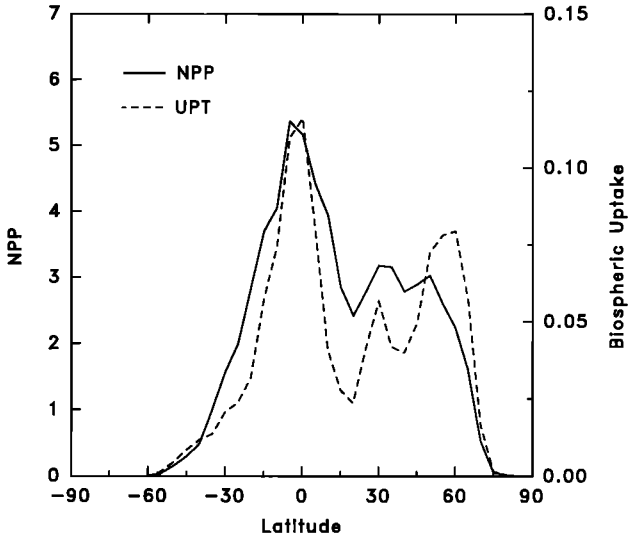

Figure 5. Latitudinal distribution of NPP (solid line) and net biospheric uptake (dashed line) for experiment 1 Units are gigatons carbon per year per 5° latitudinal band

(β_{NPP} constant). One would expect proportionality between these two curves if the biospheric uptake were proportional to NPP. The geographical variability of NPP and the turnover times leads to a "bimodal" curve for the net biospheric uptake, showing a first maximum in tropical regions due to high NPP, but also a second maximum at 60°N due to the slow turnover time of mid- and high-latitude ecosystems. The assumption often made that NPP and CO_2 fertilization sink should match spatially [*Heimann and Keeling,* 1989; *Tans et al.,* 1990; *Enting et al.,* 1993] implies that the lag between NPP and respiration is constant, that is, that the soil turnover time is a constant independent of climate, vegetation and soil type, which is extremely doubtful.

Experiment 1 gives, with a constant β_{NPP} of 0.35, a cumulative biospheric uptake of 43 Gt C on the period 1850–1990. For the same time period, the Siegenthaler and Sarmiento's integrated missing sink amounts to 97 Gt C, and is completely explained by other global carbon cycle models with the same value of β. Again, the reason for the discrepancy between our result and previous studies [e.g., *Keeling et al.,* 1989a] is clearly because our β formulation is applied to NPP and not to NEP, that is, the βs are not equivalent. As shown before (Figure 1), a β_{NPP} formulation allows respiration flux increases to catch up the NPP increases, whereas, by definition, a β_{NEP} formulation will produce an increasing uptake ad infinitum. Therefore the effective uptake is much smaller for an β_{NPP}.

Inclusion of limitations (water, nitrogen, and phosphorus) in the formulation of β (experiment 2-6) will affect the distribution of the biospheric sink and increase the spatial mismatch between NPP and net biospheric uptake. The distribution of β_{rel} (Plate 1) varies from 0 to 1.5, with β decreasing with increasing latitude (due to lower temperature inducing low mineral nitrogen availability). Arid regions (Saharian desert and Middle Eastern semidesert, Australian grasslands, Mediterranean shrubs) have a slightly higher β than the surrounding regions, reflecting the increase of water use efficiency with increasing atmospheric CO_2. These features are qualitatively similar to other modeling results [*Woodward and Smith,* 1995; *Melillo et al.,* 1993; *Shaver et al.,* 1992]. Tropical rain forests (especially in South America) show a lower β than adjacent regions due to phosphorus limitations.

As we mentioned before, the mathematical formulation used to express the relation between NPP and at-

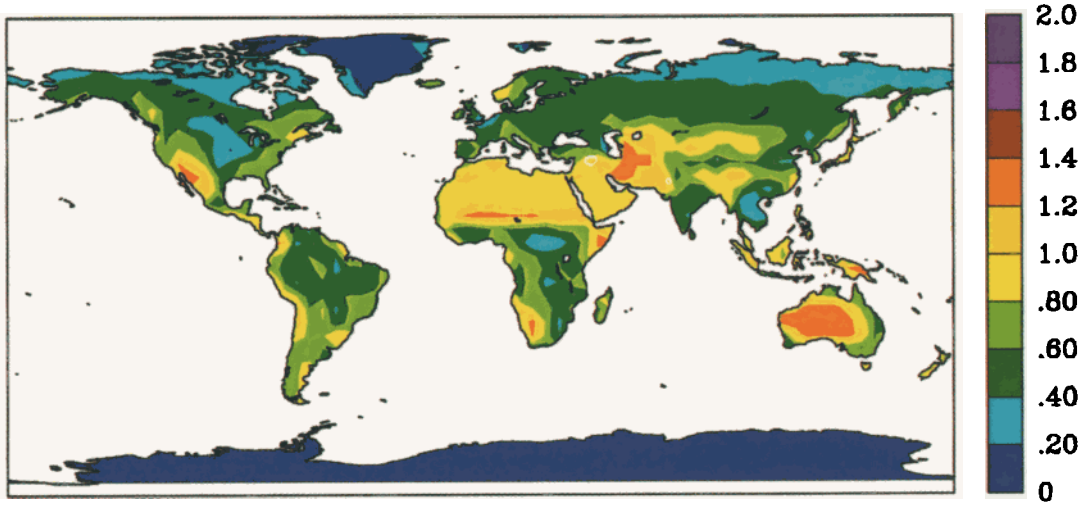

Plate 1. Modeled distribution of β_{rel} See text for explanations

mospheric CO_2 ((4),(15), and (16)) is not crucial to the spatial and temporal distribution of the biospheric sink. For the 1850–1990 time series, the use of a rectangular hyperbolic (experiment 2), linear (experiment 5), and logarithmic (experiment 6) function resulted in almost identical biospheric sinks: their differences are within 5% of their mean. For the time interval we investigated, the CO_2 increase (from 280 to 350 ppmv) was not large enough for the mathematical elaborate formulations we explored to produce important departure from a simple linear relationship between NPP and CO_2.

Implications for the Carbon Budget

In experiment 2, we tried to explain the entire time series of the residual missing sink with the fertilization effect. For that purpose, using the β formulation described before ((16) and (22)), we calculated the year to year biospheric uptake, adjusting the scaling factor α_{calib} for $T_{calib} = 1990$ (25).

As one can see in Figure 6, the residual missing sink from *Siegenthaler and Sarmiento* [1993] increases almost linearly until 1925. Then, it builds up rapidly, but most of the accumulation occurs over the last 40 years. The integrated sink is 8 Gt C in 1900 and increases by 9, 27, and 53 Gt C in each of the 30-year periods from 1901 to 1930, 1931 to 1960, and 1961 to 1990, respectively. We also note a slightly reduced sink for the last decade of the time series.

Conversely, the modeled increase in biospheric uptake simply follows, with a delay, the atmospheric CO_2 build-up (12) The modeled annual sink is therefore slightly lower than the residual sink during the nineteenth century, greatly overestimated for the 1900–1950 period, but underestimated again for the 1960–1980 period.

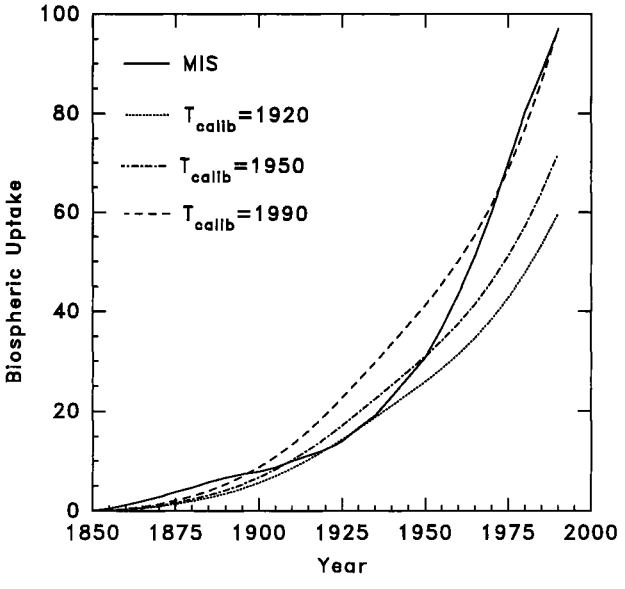

Figure 6. Time series of cumulated residual missing sink (F_{MIS}, solid line), and modeled cumulative biospheric uptake for experiments 2 to 4 with $T_{calib} = 1990$ (dashed line), 1950 (dash-dotted line) and 1920 (dotted line), respectively. Units are gigatons carbon.

Part of this discrepancy may reside in the uncertainties in the deforestation time series [*Houghton,* 1991] used to derive the missing sink. The land use change flux is the component of the carbon budget with the largest uncertainty (about 30 %). Present-day land use change flux estimation may be too high in the tropics [*Skole and Tucker,* 1993] and in the mid latitudes [*Dixon et al.,* 1994].

The main reason for disagreement between the modeled and observed missing sink is certainly due to the hypothesis we made, that the missing sink has to be explained by the fertilization effect only. In that sense, our results are qualitatively similar to those of *Enting and Mansbridge* [1987] and *Enting* [1992] which clearly document the incompatibility between atmospheric CO_2 time series and any oceanic or terrestrial uptake driven only by the increase of atmospheric CO_2. Therefore the sink should be sought in a mechanism at least partially independent of the atmospheric CO_2 build-up. Results from experiment 2 highlight that other effects like climate variability and its impact on terrestrial fluxes, oceanic fluxes, atmospheric nitrogen deposition on land and ocean may also play a role in the carbon budget closure more significantly than previously thought [*Dai and Fung,* 1993; *Keeling et al.,* 1995; *Peterson and Melillo,* 1985; *Schindler and Bayley,* 1993]. We therefore carried out experiments 3 and 4, recalculating the modeled biospheric uptake with T_{calib} scaled to 1950 and 1920, respectively (25). In other words, CO_2 fertilization is required to explain the entire sink from 1850 up to T_{calib}. The reasons for these dates are the following: 1950 corresponds to the restart of the world economy after World War II, the exponential growth of transportation, and the subsequent switch from a coal industry to a petroleum economy [*Rotty,* 1981]. Nitrogen emissions due to fossil fuel consumption have dramatically increased around that time as NO_x emission ratio is much higher for petroleum than for coal [*Logan,* 1983; *Müller,* 1992]. The choice of 1920 as a second crucial time in the biosphere evolution is suggested by the work of *Dai and Fung* [1993], where they showed the potential importance of climatic variability on the net exchange of CO_2 between the atmosphere and the biosphere, and that one can have sufficient confidence in the climatic record after 1920.

Integrated biospheric uptakes for the three experiments 2, 3, and 4 are shown in Figure 6. As already mentioned, the modeled uptake in experiment 2 ($T_{calib} = 1990$) overestimates the sink for the median part of the time series and underestimates it later. This

implies the need for an additional source during the 1900–1930s and an additional sink for the 1960–1970s. In other words, land use modification and CO_2 fertilization effect are not likely to be the only two biospheric processes altering the atmospheric CO_2 abundance. If they were, that would imply a stronger than believed land use change in the time period prior to 1940 and a reduced deforestation flux in the recent years. While there is some satellite-derived evidence for a weaker deforestation source in the 1980s than the Houghton estimate [*Skole and Tucker*, 1993], these results suggest a reexamination of the history of the land use modification. However, the only two ways to improve the agreement between the deconvoluted and the calculated biospheric sink are to either increase the land use source or to reduce the oceanic uptake. Both cases would lead to a larger deconvoluted biospheric sink, which in turn would require an even more effective CO_2 fertilization uptake than what assumed in experiment 2. As we will show below, this is ecophysiologically hardly sustainable.

We note that this study has kept the present-day distribution of cultivation [*Matthews*, 1983] constant for the entire integration period. As cultivated area is short-term carbon storage, it does not contribute substantially to the biospheric sink. This study therefore underestimates the sink for most of the time period. Furthermore, given the likelihood of nitrogen fertilization, we suggest that a conservative case like in the experiments 3 (T_{calib} = 1950) or 4 (T_{calib} = 1920) is more likely.

We note that the actual global mean values of β_{NPP}, calculated as

$$\beta_{NPP} = \frac{(NPP_{1990} - NPP_{1850})/NPP_{1850}}{(C_{1990} - C_{1850})/C_{1850}} \quad (26)$$

amounts to 0.68, 0.49, and 0.40 for experiments 2, 3, and 4, respectively (Table 3). When computed for each ecosystem, (26) leads to relatively high values of β_{NPP} for most of the ecosystems, for experiment 2 (Table 3): all ecosystems other than tundra and ice desert have a mean value of β higher than 0.5. That would mean a 50% increase of NPP for a CO_2 doubling. Although there are still large uncertainties about the actual range of β, such a high response lacks experimental support. Experiments 3 and 4 give more realistic values for β.

Table 3 shows a factor of 2 difference among βs of the different ecosystems, as a result of the spatial variations of the turnover times and limiting factors. Also, as has been demonstrated in Figure 1, β_{NPP} is larger than β_{NEP} by a factor of about 3.

For experiments 3 and 4, the 1850–1990 integrated modeled uptake amounts to 72 and 60 Gt C, corresponding to 74 and 62 % of the integrated missing sink, respectively (Table 4). The mean calculated uptake is 2.0, 1.4, and 1.2 Gt C/yr for experiments 2 to 4, respectively, for the decade of the 1980s (Table 4). For that time period, the Siegenthaler and Sarmiento's estimate is 1.7 Gt C/yr for the missing sink. In other words, the T_{calib} = 1950 and T_{calib} = 1920 experiments leave 25 and 37 % of the missing sink unexplained, so that atmospheric nitrogen deposition on land and ocean, climatic variability, or other mechanisms would have to account for the remainder.

The implications of this study for the future is important. One of the aims of the IPCC [*Intergovernmental*

Table 3. Vegetation-Type Variability of β_{NPP} and β_{NEP} for the First Four Experiments Described in Table 2

Vegetation Type [a]	Experiment 1		Experiment 2		Experiment 3		Experiment 4	
	β_{NEP} [b]	β_{NPP} [c]	β_{NEP}	β_{NPP}	β_{NEP}	β_{NPP}	β_{NEP}	β_{NPP}
1	0.14	0.40	0.25	0.71	0.15	0.52	0.13	0.43
2	0.15	0.40	0.25	0.65	0.19	0.46	0.15	0.38
3	0.15	0.40	0.22	0.58	0.16	0.41	0.13	0.34
4	0.12	0.40	0.22	0.80	0.17	0.59	0.14	0.49
5	0.12	0.40	0.21	0.71	0.16	0.51	0.13	0.42
6	0.10	0.40	0.15	0.61	0.11	0.44	0.09	0.36
7	0.09	0.40	0.12	0.49	0.08	0.35	0.07	0.28
8	0.10	0.40	0.23	0.91	0.17	0.69	0.14	0.57
9	0.09	0.40	0.08	0.31	0.06	0.21	0.05	0.17
10	0.13	0.40	0.21	0.61	0.15	0.44	0.13	0.36
Global	0.12	0.40	0.21	0.68	0.15	0.49	0.12	0.40

For β_{NPP} see equation 26, and β_{NEP} is defined as $[(B_{1990} - B_{1850})/B_{1850}]/[(C_{1990} - C_{1850})/C_{1850}]$.
[a] Vegetation Type Numbering is as in Table 1.
[b] Note that a constant β_{NPP} does not imply a constant β_{NEP}.
[c] Corresponding β_{hyp} for a β_{lin} = 0.35.

Panel on Climate Change (IPCC), 1990; 1992; 1994] is to predict future atmospheric CO_2 levels and related future fossil fuel emissions. Two sets of calculations are designed for the 1995 IPCC report [*Enting and Lassey,* 1993; *Enting et al.,* 1994]. The first set directly calculates future atmospheric CO_2 concentration for specified anthropogenic emissions, whereas the second set (inverse calculations) calculates the emissions required to achieve a given atmospheric CO_2 stabilization. Both approaches make use of global carbon models to calculate ocean and terrestrial uptakes. To perform these calculations, modelers need to have a balanced CO_2 budget, that is, all IPCC models have a CO_2 fertilization function adequately tuned to give a zero missing sink for the 1765–1990 time series of CO_2 [*Enting et al.,* 1994]. Therefore the resultant conclusions are based on the hypothesis that the present-day missing sink is entirely explained by the CO_2 fertilization effect.

If CO_2 fertilization explains only a fraction of the missing sink, the IPCC scenarios would overestimate the role of the biosphere. This would, in turn, underestimate the atmospheric CO_2 levels in the forward scenarios, or overestimate the inferred fossil fuel emission rates in the inverse scenarios. As an example, we calculated with SLAVE the biospheric uptake for the IPCC inverse scenario S650 (stabilization at 650 ppmv), β being scaled to T_{calib} = 1920, 1950, and 1990 (Figure 7). The T_{calib} = 1990 experiment leads to a biospheric uptake almost twice as large as the T_{calib} = 1920. For the year 2100, the uptake with T_{calib} = 1990 is 6 Gt C whereas it is only 3.6 Gt C with T_{calib} = 1920. That means that for the stabilization, the fossil fuel release allowed with such an efficient biosphere would be much larger than the one indicated if other factors contribute to the biospheric sink.

Conclusions

This modeling approach has emphasized several important features of the global carbon cycle. The CO_2 fertilization effect as the major mechanism to explain the missing sink is examined here.

When estimating the fertilization effect, it is of prior importance to explicitly mention the mathematical formalism adopted. We highlighted three sources of confusion: the ecological variable to which the fertilization function is applied, the mathematical relation between this variable and atmospheric CO_2, and the geographical distribution of the fertilization factor.

The 1850–1990 time series of the missing sink has been obtained by deconvolution of the ice core CO_2 data. This time series reveals that the fertilization effect, as modeled here, cannot explain the entirety of the missing sink, as the missing sink from deconvolution does not follow the atmospheric CO_2 increase as the modeled uptake does. Our estimate is that two thirds to three fourths of the integrated missing sink is due to CO_2 greening of the biosphere. Other candidates like nitrogen deposition, climatic variability, or mid latitude forest regrowth may eventually fill the gap. Furthermore, increased nitrogen availability, and climatic variability can modulate the fertilization effect through biospheric feedbacks.

This result is consistent with the analyses by Enting and coworkers [*Enting and Mansbridge,* 1987; *Enting,* 1992]. One cannot explain the recent history of atmospheric CO_2 with the prescribed fossil fuel release and land use modification, and a linear steady state ocean biosphere system. However, *Enting* [1992] concludes that allowing for a fertilization effect increases the discrepancy between the ice core data and the cal-

Table 4. Comparison of the Deconvoluted Biospheric Sink, F_{MIS}, With the CO_2 Fertilization Sink, F_{FER}, Calculated in the Six Experiments Described in Table 2

Experiment	$\int F_{FER}$, Gt C [(a)]	$\frac{\int F_{FER}}{\int F_{MIS}}$, %	$F_{FER}(80s)$, Gt C/yr	$\frac{F_{FER}(80s)}{F_{MIS}(80s)}$, %
1	43	44	0.87	51
2	97	100	2.0	118
3	72	74	1.4	82
4	60	62	1.2	70
5	97	100	2.04	121
6	97	100	1.95	115

Calculated 1850–1990 integrated biospheric uptake ($\int F_{FER}$), fraction of the integrated residual explained by CO_2 fertilization uptake ($\int F_{FER}/\int F_{MIS}$), calculated mean biospheric uptake for the 1980s ($F_{FER}(80s)$), and fraction of the 1980s mean residual explained by CO_2 fertilization uptake ($F_{FER}(80s)/F_{MIS}(80s)$). In columns 3 and 5, the integrated residuals and the 1980s mean residual were obtained by deconvolution [*Siegenthaler and Sarmiento,* 1993].
(a) See equation 25.

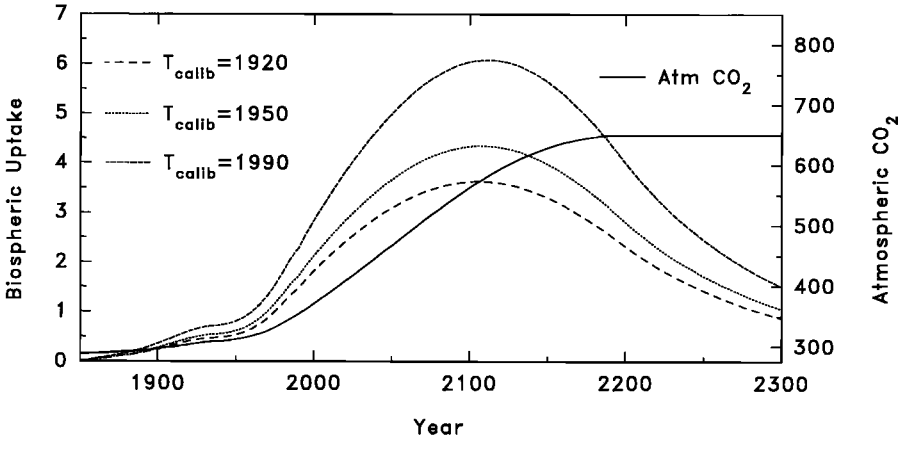

Figure 7. IPCC S650 scenario of future stabilization CO_2 concentration (part per million by volume) (solid line), and modeled annual biospheric uptake for experiments 2 to 4 (gigatons carbon per year) (dashed, dash-dotted, and dotted lines, respectively).

culated estimate. His "best fit" is obtained with a static biosphere ($\beta = 0$), the ocean being the only CO_2 sink. With the oceanic uptake estimated it a priori from the Geophysical Fluid Dynamics Laboratory three-dimensional model [*Sarmiento et al.*, 1992], we conclude that the CO_2 fertilization effect can acount for a non zero fraction, but not 100%, of the residual sink.

Note that the *Enting* [1992] fit to the atmospheric CO_2, with the help of the fertilization effect, is imposed along the entire ice core time series (1700 up to present). In this study, we show that, for the entire time series (1850–1990), the agreement between modelled uptake and deconvoluted missing sink is weak, regardless of the experiment adopted. But, if one limits the fit to a fraction of the time series (i.e., 1850–1920, or 1850–1950), the agreement is significantly improved.

When compared to the other studies which attempted to reconstruct the time evolution of the carbon cycle [e.g., *Enting and Mansbridge*, 1987; *Keeling et al.*, 1989a; *Enting*, 1992; *Siegenthaler and Sarmiento*, 1993] our approach presents an innovative difference. This study is the first to make use of a global biospheric model to estimate the biospheric contribution to the carbon cycle over the industrial period. The studies mentioned herinabove estimated the fertilization flux from a simple one-box model. This study shows that the spatial distribution of the net biospheric uptake does not match the distribution of equilibrium NPP. The fertilization effect has its own spatial distribution, and is a function of NPP, carbon residence time in the biosphere, and the availability of water, nitrogen, and other controlling factors.

Acknowledgments. The authors are grateful to P. Vitousek, H. Mooney, C. Field, I. Enting, and J.-F. Müller for particularly useful discussion, and to the reviewers for helpful comments on the manuscript. We also wish to thank J. Sarmiento for providing us with the time series of carbon budget fluxes. Financial support for PF comes from the Belgian Institute for Encouragement of Industrial and Agricultural Scientific Research. IF and JJ are supported by NASA, Office of Mission to Planet Earth and the U.S. Department of Energy Carbon Dioxide Program. The National Center for Atmospheric Research is sponsored by the National Science Foundation.

References

Andres, R. J., G. Marland, T. Boden, and S. Bischoff, Carbon dioxide emissions from fossil fuel combustion and cement manufacture 1751–1991 and an estimate of their isotopic composition and latitudinal distribution, in *The Carbon Cycle*, edited by T. M. L. Wigley and D. S. Schimel, UCAR/Off. for Interdisciplinary Earth Stud., Boulder, Colo., in press, 1995.

Bacastow, R., and C. D. Keeling, Atmospheric carbon dioxide and radiocarbon in the natural carbon cycle, II, Changes from A.D. 1700 to 2070 as deduced from a geochemical reservoir, in *Carbon and the Biosphere*, edited by G. M. Woodwell and E. V. Pecan, pp. 86–135, U.S. Dep. of Comm., Springfield, Va., 1973.

Bazzaz, F. A., The response of natural ecosystems to the rising global CO_2 levels, *Annu. Rev. Ecol. Syst.*, *21*, 167–196, 1990.

Bolin, B., B. R. Döös, J. Jäger, and R. A. Warrick, (Eds.), *The Greenhouse Effect, Climatic Change and Ecosystems, SCOPE 29*. John Wiley, New York, 1986.

Bouwman, A. F., Global distribution of the major soils and land cover types, in *Soil and the Greenhouse Effect*, edited

by A. F. Bouwman, pp. 33–59, John Wiley, New York, 1990.

Ciais, P., P. Tans, J. W. White, M. Trolier, R. Francey, J. Berry, D. Randall, P. Sellers, J. Collatz, and D. Schimel, Partitioning of ocean and land uptake of CO_2 as inferred by $\delta^{13}C$ measurements from the NOAA Climate Monitoring and Diagnostics Laboratory Global Air Sampling Network, *J. Geophys. Res.*, *100*, 5051–5070, 1995.

Dai, A., and I. Fung, Can climate variability contribute to the missing CO_2 sink?, *Global Biogeochem. Cycles*, *7*, 599–609, 1993.

Dixon, R. D., S. Brown, R. A. Houghton, A. M. Solomon, M. C. Trexler, and J. Wisniewski, Carbon pools and flux of global forest ecosystems, *Science*, *263*, 185–190, 1994.

Enting, I. G., The incompatibility of ice-core CO_2 data with reconstructions of biotic CO_2 sources, II, The influence of CO_2 fertilised growth, *Tellus*, *44B*, 23–32, 1992.

Enting, I. G., and K. R. Lassey, Projections of future CO_2, *Tech. Rep.* 27, Div. of Atmos. Res., CSIRO, Australia, 1993.

Enting, I. G., and J. V. Mansbridge, The incompatibility of ice-core CO_2 data with reconstructions of biotic CO_2 sources, *Tellus*, *39B*, 318–325, 1987.

Enting, I. G., C. M. Trudinger, R. J. Francey, and H. Granek, Synthesis inversion of atmospheric CO_2 using the GISS tracer transport model, *Tech. Rep.* 29, Div. of Atmos. Res., CSIRO, Australia, 1993.

Enting, I. G., T. M. L. Wigley, and M. Heimann, Future emissions and concentrations of carbon dioxide: Key Ocean/Atmosphere/Land Analyses, *Tech. Rep.* 31, Div. of Atmos. Res., CSIRO, Australia, 1994.

Esser, G., Sensitivity of global carbon pools and fluxes to human and potential climatic impacts, *Tellus*, *39*, 245–260, 1987.

Farquhar, G. D., S. von Caemmerer, and J. A. Berry, A biochemical model of photosynthetic CO_2 assimilation in leaves of C_3 species, *Planta*, *149*, 78–90, 1980.

Food and Agricultural Organization (FAO), Soil map of the world 1:5000000, *Tech. Rep.*, vol. I-X, Food and Agricult. Org., Rome, 1974-1982.

Francey, R. J., P. P. Tans, C. E. Allison, I. G. Enting, J. W. White, and M. Trolier, Changes in oceanic and terrestrial carbon uptake since 1982, *Nature*, *373*, 326–330, 1995.

Friedlingstein, P., C. Delire, J.-F. Müller, and J.-C. Gérard, The climate induced variation of the continental biosphere: A model simulation of the Last Glacial Maximum, *Geophys. Res. Lett.*, *19*, 897–900, 1992.

Friedlingstein, P., J.-F. Müller, and G. P. Brasseur, Sensitivity of the terrestrial biosphere to climate changes: Impact on the carbon cycle, *Environ. Pollut.*, *83*, 143–146, 1994.

Gates, D. M., Global biospheric response to increasing atmospheric carbon dioxide concentration, in *Direct Effect of Increasing Carbon Dioxide on Vegetation*, edited by B. R. Strain and J. D. Cure, pp. 171–184, U.S. Dep. of Energy, DOE/ER-0238, Washington, D. C., 1985.

Gifford, R. M., Interaction of carbon dioxide with growth-limiting environmental factors in vegetation productivity: Implications for the global carbon cycle, *Adv. Bioclimatol.*, *1*, 24–58, 1992.

Goudriaan, J., and P. Ketner, A simulation study for the global carbon cycle, Including man's impact on the biosphere, *Clim. Change*, *6*, 167–192, 1984.

Heimann, M., and C. D. Keeling, A three-dimensional model of atmospheric CO_2 transport based on observed winds, 2, Model description and simulated tracer experiments, in *Aspects of Climate Variability in the Pacific and the Western Americas, Geophys. Monogr. Ser.*, Vol. 55, edited by D. H. Peterson, pp. 237–275, AGU, Washington, D. C., 1989.

Houghton, R. A., Tropical deforestation and atmospheric carbon dioxide, *Clim. Change*, *19*, 99–118, 1991.

Houghton, R. A., Is carbon accumulating in the northern temperate zone?, *Global Biogeochem. Cycles*, *7*, 611–617, 1993.

Hudson, R. J. M., S. A. Gherini, and R. A. Goldstein, Modeling the global carbon cycle: Nitrogen fertilization of the terrestrial biosphere and the "missing" CO_2 sink, *Global Biogeochem. Cycles*, *8*, 307–333, 1994.

Intergovernmental Panel on Climate Change (IPCC), *Climate Change, the IPCC Scientific Assessment*, edited by J. T. Houghton, G. J. Jenkins, and J. J. Ephraums. Cambridge University Press, New York, 1990.

Intergovernmental Panel on Climate Change (IPCC), *The Supplementary Report to the IPCC Scientific Assessment*, edited by J. T. Houghton, B. A. Callander, and S. K. Varney. Cambridge University Press, New York, 1992.

Intergovernmental Panel on Climate Change (IPCC), *Climate Change 1994, Radiative Forcing of Climate Change and Evaluation of the IPCC IS92 Emission Scenarios*, edited by J. T. Houghton, L. Meira Filho, J. Bruce, Hoesung Lee, B. A. Callander, E. Haites, N. Harris, and K. Maskell. Cambridge University Press, New York, 1994.

Keeling, C. D., R. B. Bacastow, A. F. Carter, S. C. Piper, T. P. Whorf, M. Heimann, W. G. Mook, and H. Roeloffzen, A three-dimensional model of atmospheric CO_2 transport based on observed winds, 1, Analysis on observational data, in *Aspects of Climate Variability in the Pacific and the Western Americas, Geophys. Monogr. Ser.*, Vol. 55, edited by D. H. Peterson, pp. 165–236, AGU, Washington, D. C., 1989a.

Keeling, C. D., S. C. Piper, and M. Heimann, A three-dimensional model of atmospheric CO_2 transport based on observed winds, 4, Mean annual gradients and interannual variations, in *Aspects of Climate Variability in the Pacific and the Western Americas, Geophys. Monogr. Ser.*, Vol. 55, edited by D. H. Peterson, pp. 305–363, AGU, Washington, D. C., 1989b.

Keeling, C. D., S. C. Piper, and T. Whorf, Interpretation of the modern CO_2 concentration record using three-dimensional and compartment models, in *The Carbon Cycle*, edited by T. M. L. Wigley and D. S. Schimel, UCAR/Off. for Interdisciplinary Earth Stud., Boulder, Colo., in press, 1995.

Kohlmaier, G. H., H. Bröl, E. O. Siré, M. Plöchl, and R. Revelle, Modelling estimates of plants and ecosystem response to present levels of excess CO_2, *Tellus*, *39B*, 155–170, 1987.

Kohlmaier, G. H., E. O. Siré, A. Janecek, C. Keeling, S. Piper, and R. Revelle, Modelling the seasonal contribution of a CO_2 fertilization effect of the terrestrial veg-

etation to the amplitude increase in atmospheric CO_2 at Mauna Loa Observatory, *Tellus, 41B*, 487–510, 1989.

Körner, C., CO_2 fertilization: The great uncertainty in future vegetation development, in *Vegetation Dynamics and Global Change*, edited by A. M. Solomon and H. H. Shugart, pp. 53–70, Chapman and Hall, New York, 1993.

Körner, C., and J. A. Arnone, Responses to elevated carbon dioxide in artificial tropical ecosystems, *Science, 257*, 1672–1675, 1992.

Lieth, H., Modeling the primary productivity of the world, in *Primary Productivity of the Biosphere*, edited by H. Lieth and R. H. Whittaker, pp. 237–263, Springer-Verlag, New York, 1975.

Logan, J. A., Nitrogen oxides in the troposphere: Global and regional budgets, *J. Geophys. Res., 88*, 10,785–10,807, 1983.

Matthews, E., Global vegetation and land use: New high-resolution data bases for climate studies, *J. Clim. Appl. Meteorol., 22*, 474–487, 1983.

McGuire, A. D., J. M. Melillo, L. A. Joyce, D. W. Kicklighter, A. L. Grace, B. Moore, and C. J. Vörösmarty, Interactions between carbon and nitrogen dynamics in estimating net primary productivity for potential vegetation in North America, *Global Biogeochem. Cycles, 6*, 101–124, 1992.

Melillo, J. M., J. D. Aber, and J. F. Muratore, Nitrogen and lignin control of hardwood leaf litter decomposition dynamics, *Ecology, 63*, 621–626, 1982.

Melillo, J. M., R. J. Naiman, J. D. Aber, and K. Eshleman, The influence of substrate quality and stream size on wood decomposition dynamics, *Oecologia, 58*, 281–285, 1983.

Melillo, J. M., R. J. Naiman, J. D. Aber, and A. E. Linkins, Factors controlling mass loss and nitrogen dynamics of plant litter decaying in northern streams, *Bull. Mar. Sci., 35*, 341–356, 1984.

Melillo, J. M., A. D. McGuire, D. W. Kicklighter, B. Moore, C. J. Vorosmarty, and A. L. Schloss, Global climate change and terrestrial net primary production, *Nature, 363*, 234–240, 1993.

Mooney, H. A., B. G. Drake, R. J. Luxmoore, W. C. Oechel, and L. F. Pitelka, Predicting ecosystem responses to elevated CO_2 concentrations, *BioScience, 41*, 96–104, 1991.

Müller, J.-F., Geographical distribution and seasonal variation of surface emissions and deposition velocities of atmospheric trace gases, *J. Geophys. Res., 97*, 3787–3804, 1992.

Norby, R. J., C. A. Gunderson, S. D. Wullschleger, E. G. O'Neill, and M. K. McCracken, Productivity and compensatory responses of yellow-poplar trees in elevated CO_2, *Nature, 357*, 322–324, 1992.

Oechel, W., and B. R. Strain, Native species responses to increased carbon dioxide concentration, in *Direct Effect of Increasing Carbon Dioxide on Vegetation*, edited by B. R. Strain and J. D. Cure, pp. 117–154, U.S. Dep. of Energy, DOE/ER-0238, Washington, D. C., 1985.

Oechel, W. C., S. Cowles, N. Grulke, S. J. Hastings B. Lawrence, T. Prudhomme, G. Riechers, B. Strain, D. Tissue, and G. Vourlitis, Transient nature of CO_2 fertilization in Arctic tundra, *Nature, 371*, 500–503, 1994.

Parton, W. J. et al., Observations and modeling of biomass and soil organic matter dynamics for the grassland biome worldwide, *Global Biogeochem. Cycles, 7*, 785–809, 1993.

Pastor, J., and W. M. Post, Influence of climate, soil moisture and succession on forest carbon and nitrogen cycles, *Biogeochemistry, 2*, 3–27, 1986.

Peterson, B. J., and J. M. Melillo, The potential storage of carbon caused by eutrophication of the biosphere, *Tellus, 37*, 117–127, 1985.

Polglase, P. J., and Y. P. Wang, Potential CO_2-enhanced carbon storage by the terrestrial biosphere, *Aust. J. Bot., 40*, 641–656, 1992.

Polley, H. W., H. B. Johnson, B. D. Marino, and H. S. Mayeux, Increase in C_3 plant water-use efficiency and biomass over glacial to present CO_2 concentrations, *Nature, 361*, 61–63, 1993.

Quay, P. D., B. Tilbrook, and C. S. Wong, Oceanic uptake of fossil fuel CO_2: Carbon-13 evidence, *Science, 256*, 74–79, 1992.

Raich, J. W., E. B. Rastetter, J. M. Melillo, D. W. Kicklighter, P. A. Steudler, B. J. Peterson, A. L. Grace, B. Moore, and C. J. Vörösmarty, Potential net primary productivity in South America: Application of a global model, *Ecol. Appl., 4*, 399–429, 1991.

Rotty, R. M., Data for global CO_2 production from fossil fuels and cement, in *Carbon Cycle Modelling, SCOPE 16*, edited by B. Bolin, pp. 315–332, John Wiley, New York, 1981.

Sarmiento, J. L., Atmospheric CO_2 stalled, *Nature, 365*, 697–698, 1993.

Sarmiento, J. L., J. C. Orr, and U. Siegenthaler, A perturbation simulation of CO_2 uptake in an ocean general circulation model, *J. Geophys. Res., 97*, 3621–3645, 1992.

Schindler, D. W., and S. E. Bayley, The biosphere as an increasing sink for atmospheric carbon: Estimate from increased nitrogen deposition, *Global Biogeochem. Cycles, 7*, 717–733, 1993.

Schlesinger, W. H., *Biogeochemistry: An Analysis of Global Change*. Academic, San Diego, Calif., 1991.

Sellers, P. J., D. A. Randall, G. J. Collatz, J. Berry, C. Field, D. A. Dazlich, and C. Zhang, A revised land-surface parameterization (SiB2) for atmospheric GCMs, I, Model formulation, *J. Clim.*, , in press, 1995.

Shaver, G. R., W. D. Billings, F. Stuart Chapin, A. E. Giblin, K. J. Nadelhoffer, W. C. Oechel, and E. B. Rastetter, Global change and the carbon balance of arctic ecosystems, *BioScience, 42*, 433–441, 1992.

Shea, D. J., Climatological atlas: 1950-1979, *Tech. Rep. NCAR/TN-269+STR* , Nat. Cent. for Atmos. Res., Boulder, Colo., 1986.

Siegenthaler, U., and J. L. Sarmiento, Atmospheric carbon dioxide and the ocean, *Nature, 365*, 119–125, 1993.

Skole, D., and C. Tucker, Tropical deforestation and habitat fragmentation in the Amazon: Satellite data from 1978 to 1988, *Science, 260*, 1905–1910, 1993.

Strain, B. R., and J. D. Cure, *Direct Effects of Increasing Carbon Dioxide on Vegetation*. U.S. Dep. of Energy, DOE/ER–0238, Washington, D.C., 1985.

Tans, P. P., I. Y. Fung, and T. Takahashi, Observational constraints on the global atmospheric CO_2 budget, *Science, 247*, 1431–1438, 1990.

Tans, P. P., J. A. Berry, and R. F. Keeling, Oceanic $^{13}C/^{12}C$ observations: A new window on oceanic CO_2 uptake, *Global Biogeochem. Cycles*, *7*, 353–358, 1993.

Townsend, A. R., B. H. Braswell, E. A. Holland, and J. E. Penner, Nitrogen deposition and terrestrial carbon storage: Linking atmospheric chemistry and the global carbon budget, *Ecol. Appl.*, , in press, 1995.

Vitousek, P. M., and R. W. Howarth, Nitrogen limitation on land and in the sea: How can it occur?, *Biogeochemistry*, *13*, 87–115, 1991.

Vitousek, P. M., and R. L. Sanford, Nutrient cycling in moist tropical forest, *Annu. Rev. Ecol. Syst.*, *17*, 137–167, 1986.

Vitousek, P. M., T. Fahey, D. W. Johnson, and M. J. Swift, Element interactions in forest ecosystems: Succession, allometry and input-output budgets, *Biogeochemistry*, , 7–34, 1988.

Warnant, P., L. François, D. Strivay, and J.-C. Gérard, CARAIB: A global model of terrestrial biological productivity, *Global Biogeochem. Cycles*, *8*, 255–270, 1994.

Woodward, F. I., Stomatal numbers are sensitive to increase in CO_2 from pre-industrial levels, *Nature*, *327*, 617–618, 1987a.

Woodward, F. I., and T. M. Smith, Climate-related impacts on the terrestrial carbon cycle, in *The Carbon Cycle*, edited by T. M. L. Wigley and D. S. Schimel, UCAR/Off. for Interdisciplinary Earth Stud., Boulder, Colo., in press, 1995.

Wullschleger, S. D., W. M. Post, and A. W. King, On the potential for a CO_2 fertilization effect in forest: Estimates of the biotic growth factor based on 58 controlled-exposure studies, in *Biotic Feedbacks in the Global Climatic System, Will the Warming Feed the Warming?*, edited by G. Woodwell and F. Mackenzie, pp. 85–107, Oxford University Press, New York, 1995.

Zobler, L., A world soil map for global climate modeling, *Tech. Rep. NASA Tech. Memo. 87802*, 1986.

G. Brasseur, D. Erickson, E. Holland, and D. Schimel, NCAR, PO Box 3000, Boulder, CO 80307 (e-mail: brasseur@acd.ucar.edu; erickson@acd.ucar.edu; eholland@acd.ucar.edu; schimel@niwot.ucar.edu).

P. Friedlingstein, I. Fung and J. John, NASA / Goddard Institute for Space Studies, 2880 Broadway, New York, NY 10025 (e-mail: pierre@dougfir.giss.nasa.gov; cxiyf@nasagiss.giss.nasa.gov; cxjgj@nasagiss.giss.nasa.gov).

(Received October 10, 1994; revised June 28, 1995; accepted August 3, 1995.)